Available online at www.sciencedirect.com
SCIENCE DIRECT
International Journal of Heat and Mass Transfer 49 (2006) 1255–1263
International Journal of HEAT and MASS TRANSFER
www.elsevier.com/locate/ijhmt

Exergetic optimization of solar collector and thermal energy storage system

F. Aghbalou [a], F. Badia [b,*], J. Illa [a]

[a] Department of Computer and Industrial Engineering, University of Lleida, C/Jaume II 69, 25001 Lleida, Spain
[b] Department of Environmental and Soil Sciences, University of Lleida, C/Jaume II 69, 25001 Lleida, Spain

Received 14 April 2004; received in revised form 10 October 2005
Available online 7 December 2005

Abstract

This paper deals with the exergetic optimization of a solar thermal energy system. This consists of a solar collector (SC) and a rectangular water storage tank (ST) that contains a phase change material (PCM) distributed in an assembly of slabs. The study takes into account both conduction and convection heat transfer mode for water in the SC, and also the phase change process for the PCM in the ST. An analytical solution for the melting process in the PCM is also presented. The results of the study are compared with previous experimental data, confirming the accuracy of the model. Results of a numerical case study are presented and discussed.

Keywords: Thermal energy storage; Analytical model; Exergy analysis; Optimization; Solar energy; Phase change materials

1. Introduction

Solar energy is an important alternative energy source for present and future use. However, the main limitations to overcome for a wide thermal solar energy use are three: (a) cost—which depends on the type and area of the solar collector (SC), (b) the performance of the necessary storage utility and (c) the quality of the stored energy, i.e., the ability of the solar installation to provide a given amount of energy at a given constant temperature, so that the higher the temperature, the higher the quality. A common solution is the use of an effective thermal energy storage system, i.e., a system able to store thermal energy at the highest possible temperature and with minimum thermal losses. The main solar thermal energy storage techniques are:

- Thermally stratified storage (sensible heat), which is an effective technique that is widely used in energy conservation and load management applications. Analytical, experimental, and numerical studies have been carried out on its performance [1–3].
- Reversible chemical heat storage which is based on the conversion of solar radiation into high-temperature heat. It consists of a closed-loop [4–6] or open-loop [7] system of reactants passing to endothermic 'solar energy storage' and exothermic 'solar energy recovery' reactors.
- Latent heat thermal energy storage. Solar energy is stored as latent heat in a phase change material (PCM). The main features of PCM are their high-energy storage density and their ability to give back the stored energy at a constant temperature. The most analysed latent heat energy storage system is the shell and tube one, with the PCM filling the shell and the heat transfer fluid flowing through the tubes [8]. A detailed discussion on the solar energy storage using PCM can be found in Aghbalou et al. [9]. In this study the energy storage is treated as a transient-continue system by using the finite difference method. The melting process of PCM was performed by using the enthalpy formulation. The PCM slabs were considered to be bathed in two different fluids.

* Corresponding author. Tel.: +34 973 702 727; fax: +34 973 702 702.
E-mail addresses: fouad@diei.udl.es (F. Aghbalou), fbadia@macs.udl.es (F. Badia), Jilla@macs.UdL.es (J. Illa).

0017-9310/$ - see front matter © 2005 Elsevier Ltd. All rights reserved.
doi:10.1016/j.ijheatmasstransfer.2005.10.014

Nomenclature

a	distance between two slabs in SEST (m)
A	area (m^2)
A_C	caption area of solar collector (m^2)
b	slab's height (m)
Bi	Biot number
C_p	constant pressure specific heat ($J\,kg^{-1}\,K^{-1}$)
E	energy (J)
Fo	Fourier number
H	enthalpy ($J\,kg^{-1}$)
h	solar collector overall heat transfer coefficient ($W\,m^{-2}\,K^{-1}$)
I	irradiation ($W\,m^{-2}$)
I_g	global solar irradiation ($W\,m^{-2}$)
I_r	irreversibility (kJ)
k	thermal conductivity ($W\,m^{-1}\,K^{-1}$)
L	latent heat ($J\,kg^{-1}$)
l	PCMs half thickness (m)
m	mass (kg)
M_0	water mass charge of solar collector (kg)
$\dot{m}$	mass flow rate ($kg\,s^{-1}$)
n	number of slabs in SEST
N	number of hours
N_{tu}	number of transfer units
Nu_j	Nusselt number at j hour
Pr	Prandtl number
q	flux (W)
Re_j	Reynolds number at j hour
T	temperature (K)
t	time (s)
U	overall heat transfer coefficient ($W\,m^{-2}\,K^{-1}$)
v	velocity ($m\,s^{-1}$)
V	volume (m^3)
V_0	volume of storage system (m^3)
x	Cartesian coordinate
W	work

Greek symbols

α	thermal diffusivity ($k/\rho C_p$) ($m^2\,s^{-1}$)
Δ	increment
δ	melted thickness (m)
ϵ	accuracy parameter
η	solar collector efficiency
θ	dimensionless temperature (T/T_{amb})
Θ	excess temperature ($T_{mean} - T(x,t)$)
μ	viscosity ($N\,s/m^2$)
ρ	density ($kg\,m^{-3}$)
ϕ	specific available energy of water
Φ	available energy of water
Ψ	fractional energy

Subscripts

analy	analytical
C	caption
cr	cross sectional
exp	experimental
g	global
in	input
j	hour index
l	liq
L	low
m	melting
mean	mean
opt	optimal
out	output
s	solid
w	water
0	initial
ς	solid or liquid state

Superscripts

k	iteration
0	initial

Zivkovic and Fujii [10] have presented a simple computational model based on enthalpy formulation for isothermal PCM encapsulated in a single container. The model was confirmed experimentally. In a recent work, Stritih [11] has studied experimentally the heat transfer problem in the solidification and melting processes of a latent heat storage system with a finned surface. Results are compared with those of heat storage unit with a flat surface.

Several methodologies for Thermal Energy Storage (TES) evaluation and comparison have been investigated [12,13] concluding that the only adequate method providing significant information is that based on the second law of thermodynamics, that is, availability analysis. Energy efficiency, i.e., the ratio of the energy returned from the storage to the energy originally delivered to the storage, does not take into account all the considerations necessary in thermal energy storage evaluation, like storage duration and temperatures of the supplied and recovered thermal energy and the surroundings. The common method of energy accounting ignores completely the quality of energy. It only tracks the quantity, which according to the first law of thermodynamics will never change. A better method for energy accounting could be based in both, first and second law of thermodynamics, which asserts that work is the highest

quality form of energy. This makes possible to identify clearer the causes and locations of thermodynamic losses.

One of the most well-known analytical solutions for moving boundary problems is the one reported by Stephan [14]. The Stephan problem considers a one-dimensional time-dependent pure conduction in a semi-infinite solid (resp. liquid) at its melting temperature (resp. solidification temperature), suddenly exposed to a surface at constant temperature. Other authors [15], have examined recently, the melting process in a two-dimensional semi-infinite PCM storage with a fin. The presented simplified analytical model based on a quasi-lineal, transient, thin-fin equation predicts the solid–liquid interface location and temperature distribution of the fin. Two regions were considered. In region 1 (resp. region 2) the heat is transferred from the wall (resp. from the fin) to the solid–liquid interface one-dimensionally in the x-direction (resp. in the y-direction). Natural convection mode transfer (resp. conduction mode transfer) is assumed to be negligible.

The purposes of this article are:

- To present a more general exergetic optimization of the solar collector, i.e., both conduction and convection heat transfer modes are considered for water. Thus, optimal output temperature and optimal mass flow rate are determined.
- To present a more general exergetic optimization of the PCM-slabs–solar energy storage tank (SEST), i.e., both optimal melting temperature and the maximum power output taking into account the phase change process are determined.
- To study the melting process in a PCM-slabs–SEST assembly by means of an analytical solution.

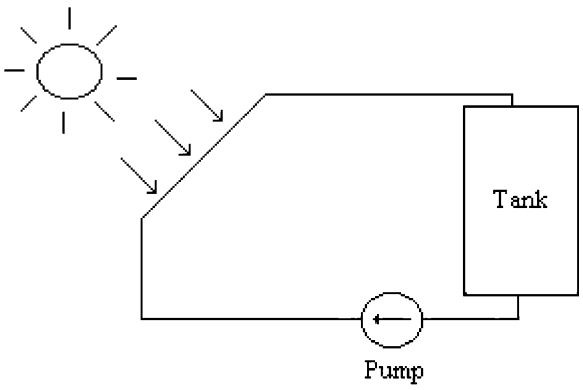

Fig. 1. General solar collector and reservoir setup.

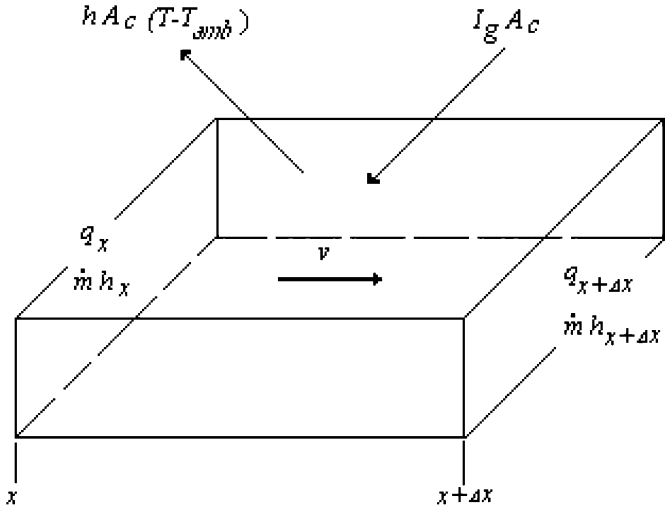

Fig. 2. Detail of the control volume used.

2. Solar collector: mathematical model and optimization

The purpose of this section is to present a method for optimizing the water mass flow rate through the solar collector in order to extract the maximum work from the solar energy (Fig. 1). This is accomplished by studying the specific available energy of water and maximising it. In the optimization procedure water output temperature is the only variable and is determined by applying the first law of thermodynamics to a representative control volume of the SC, as the one shown in Fig. 2.

The solar collector is treated as a transient-continue system, considering both conduction and convection heat transfer mode for water. Only two assumptions are done:

- The heat flux is 1-D in the x-direction.
- As the temperature range for water is not large, all thermo-physical properties of water are assumed to be constant with temperature.

The energy conservation equation written with reference to the control volume of length Δx shown in Fig. 2 contains three terms: the net rate of energy due to conduction transfer mode, the net rate of energy due to convection transfer mode, and the net rate of energy received by the absorber of the solar collector.

$$\frac{\partial T}{\partial t} = \alpha_w \frac{\partial^2 T}{\partial x^2} - v_w \frac{\partial T}{\partial x} + \frac{\eta I_g A_C}{\rho_w C_{p_w} V_{SC}} \tag{1}$$

where α_w is the thermal diffusivity; v_w is the water velocity; C_{p_w} is the water's specific heat at constant pressure; V_0 is the volume of the storage system; I_g is the global solar irradiance; A_C is the caption area; η is the solar collector efficiency defined by the expression

$$\eta I_g A_C = I_g A_C - h A_C (T - T_{amb}) \tag{2}$$

being h the solar collector's overall heat transfer coefficient and T_{amb} the ambient temperature; and ρ_w is the density of water which is related with the volume of solar collector, V_{SC}, and the solar collector's water charge, M_{SC}, by the expression

$$V_{SC} = \frac{M_{SC}}{\rho_w} \tag{3}$$

Velocity, v_w, and density, ρ_w, of water are related through expression

$$v_w = \frac{\dot{m}_w}{\rho_w A_{cr}} \tag{4}$$

where $\dot{m}_w$ is the water flow rate and A_{cr} is the tube cross sectional area.

Using the basic relation for the enthalpy variation as a function of the temperature change, $dH = mC_p dT$, corresponding to a control volume of length Δx, the following equation can be easily found:

$$v_w \frac{\partial T}{\partial x} = \frac{\dot{m}_w}{M_{SC}(T - T_{amb})} \tag{5}$$

From Eqs. (4) and (5) it can be obtained

$$\frac{\partial^2 T}{\partial x^2} = \left(\frac{\rho_w A_{cr}}{V_{SC}}\right)(T - T_{amb}) \tag{6}$$

Using Eqs. (2), (5) and (6) in Eq. (1) and arranging the terms, the following expression can be found:

$$\dot{m}_w C_{p_w} T_{amb} = \frac{\Lambda}{\theta - 1} - \Gamma - \frac{\Xi}{\theta - 1}\frac{\partial \theta}{\partial t} \tag{7}$$

where the following parameters are introduced:

$$\theta = \frac{T}{T_{amb}}$$

$$\Lambda = I_g A_C$$

$$\Gamma = \frac{A_C T_{amb} k_w}{\ell}\left[Bi - \frac{A_{cr}}{A_C}\right]$$

$$\Xi = T_{amb} M_{SC} C_{p_w}$$

$$Bi = \frac{h \times \ell}{k_w}$$

$$\ell = \frac{M_{SC}}{\rho_w A_{cr}}$$

where k_w is the thermal conductivity of water.

The specific available energy of water, ϕ, between states corresponding to temperatures T_{amb} and T is given by

$$\phi = C_{p_w} T_{amb}(\theta - 1 - \ln\theta) \tag{8}$$

Therefore, the available energy, Φ, corresponding to a given flow rate, $\dot{m}$, during an interval $[0, t]$ is

$$\Phi = \int_0^t \dot{m}(t')\phi(t')\,dt' \tag{9}$$

Substituting Eqs. (7) and (8) into Eq. (9) and applying Euler's equation [16], the dimensionless temperature θ_{opt} that maximises the available energy, Φ, can be found

$$\frac{(\theta_{opt} - 1)^3}{\theta_{opt}\ln\theta_{opt} - \theta_{opt} + 1} = \frac{\Lambda}{\Gamma} \tag{10}$$

Similar expression differing only by the right side of Eq. (10) was proposed by Bejan [17] considering only the conduction mode transfer for water.

In order to avoid water evaporation the restriction $\theta_{opt} < 100/T_{amb}$ has been imposed to the maximising procedure.

Using this result in Eq. (7) the optimal water mass flow rate, $\dot{m}_{opt}$, can be also determined.

For a given amount of solar irradiation, I, the optimal water flow rate, $\dot{m}_w$, for a given hour of a given day can be calculated form Eq. (7). Considering a complete day of energy absorption, the tank volume can be calculated. The input temperature of water in the solar collector can reasonable be assumed to be constant and equal to ambient temperature T_{amb}, as the tank will present the stratification phenomena.

3. Availability maximisation of the SEST with PCM

In order to increase the stored energy density and the quality of the stored energy, a PCM is introduced in the water tank. The thermal energy of the incoming water from the SC is released to the PCM raising its temperature. Once the melting temperature is reached, thermal energy is stored in the PCM as latent heat at constant temperature. The proposed tank in this work has a rectangular geometry and the PCM is contained in slabs of parallelepiped shape regularly distributed parallel to the stream direction, as shown in Fig. 3. This slabs can be made of thin aluminium

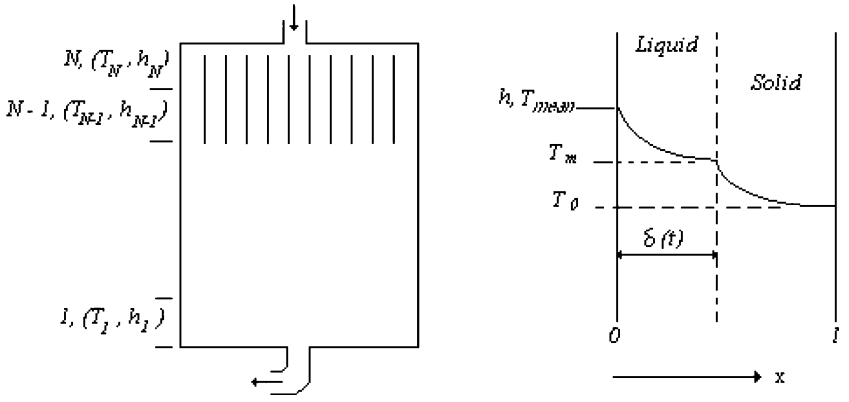

Fig. 3. PCM-slabs in tank and temperature profile in PCM-slab.

walls to ensure a good heat transfer between the water and the PCM.

This section presents a procedure to find the optimal melting temperature and the maximum power output for the PCM in the ST based on the maximisation of the availability of the SEST. This is done by assuming that the SEST behaves like a Carnot heat engine.

The main process that takes place in the ST is a heat exchange between the water coming from the solar collector and the PCM in the slabs. As the hot stream of a flow rate $\dot{m}$ at temperature T_{in} gets in contact with a PCM, a fraction of the energy of the hot stream is released to the PCM and consequently the temperature of the hot stream falls to T_{out}. Assuming both, steady state and PCM at melting temperature, T_{m}, the output temperature of the hot stream can be deduced writing the energy conservation equation for the hot stream,

$$T_{\text{out}} = T_{\text{m}} + (T_{\text{in}} - T_{\text{m}})\mathrm{e}^{-N_{\text{tu}}} \tag{11}$$

where N_{tu} is the number of transfer units, defined by expression

$$N_{\text{tu}} = \frac{UA}{\dot{m}_{\text{w}} C_{p_{\text{w}}}} \tag{12}$$

where A is the heat transfer area between the hot stream and PCM and U is the overall heat transfer coefficient. Considering that SEST with a PCM behaves like a heat engine describing a Carnot cycle, i.e., heat leaves the high temperature reservoir at temperature T_{m} and goes into the heat engine that does a certain amount of work, W, rejecting heat into the low temperature reservoir at temperature T_{L}, then, the efficiency η_{SEST} of the SEST can be expressed as

$$\eta_{\text{SEST}} = \frac{W}{\dot{m}_{\text{w}} C_{p_{\text{w}}}(T_{\text{in}} - T_{\text{out}})} = 1 - \frac{T_{\text{L}}}{T_{\text{m}}} \tag{13}$$

Substituting the expression for T_{out} found in (11) in this equation, the expression for the work done by the heat engine can be determined as

$$W = \dot{m}_{\text{w}} C_{p_{\text{w}}}(T_{\text{in}} - T_{\text{m}})\left(1 - \mathrm{e}^{-N_{\text{tu}}}\right)\left(1 - \frac{T_{\text{L}}}{T_{\text{m}}}\right) \tag{14}$$

Maximising this work the optimal melting temperature $T_{\text{m,opt}}$ for the PCM can be found

$$T_{\text{m,opt}} = (T_{\text{in}} T_{\text{L}})^{\frac{1}{2}} \tag{15}$$

This result is in agreement with the optimal latent heat storage temperature determined by Lim et al. [18]. However, their maximum power output deduced does not reflect the phase change process.

Substituting expression (15) for the optimal melting temperature in Eq. (14), the maximum output power, W_{max}, can be deduced:

$$W_{\text{max}} = \dot{m}_{\text{w}} C_{p_{\text{w}}} T_{\text{in}}\left(1 - \mathrm{e}^{-N_{\text{tu}}}\right)\left[1 - \left(\frac{T_{\text{L}}}{T_{\text{in}}}\right)^{\frac{1}{2}}\right]^2 \tag{16}$$

4. Analytical model for melting in PCM slabs

In order to complete the exergy study of SEST, the heat transfer process within the PCM has been investigated. As a result of this study, the time necessary for completely melt the PCM is obtained. This depends on boundary conditions, the geometry of the PCM slab and the thermo-physical properties of the PCM.

Heat transfer problems in PCM is a complicated subject as they show time dependence and non linear phenomena with a moving liquid–solid interface, different values for the thermo-physical properties of the solid and liquid states of the PCM, and two-dimension or three-dimension geometry. For these reasons the following assumptions have been done:

- Due to the thin thickness of PCM slabs, heat is assumed to be transferred from the walls to the liquid–solid interface in a one-dimension heat conduction transfer mode in the x-direction.
- Due to the relatively small temperature gradient, the thermo-physical properties of the PCM are assumed to be constant.

In terms of the excess temperature function $\Theta(x,t) = T_{\text{mean}} - T(x,t)$, the melting process is described by equation (see Fig. 3),

$$\frac{\partial^2 \Theta_\varsigma}{\partial x^2} = \frac{1}{\alpha_\varsigma}\frac{\partial \Theta_\varsigma}{\partial t} \tag{17}$$

where ς denotes both solid and liquid state and α_ς is the thermal diffusivity.

This equation has to be solved with initial conditions

$$t = 0, \quad \Theta_{\varsigma,0} = T_{\text{mean}} - T_0 \tag{18}$$

and boundary conditions

$$x = 0, \quad k_{\text{l}}\frac{\partial \Theta_{\text{l}}}{\partial x} = h\Theta_{\text{l}} \tag{19}$$

$$x = l, \quad \frac{\partial \Theta_{\text{s}}}{\partial x} = 0 \tag{20}$$

$$x = \delta(t), \quad \begin{cases} \Theta_\varsigma = T_{\text{mean}} - T_{\text{m}} \\ -k_{\text{l}}\frac{\partial \Theta_{\text{l}}}{\partial x} + k_{\text{s}}\frac{\partial \Theta_{\text{s}}}{\partial x} = \rho_{\text{l}} L\frac{\mathrm{d}\delta(t)}{\mathrm{d}t} \end{cases} \tag{21}$$

where $\delta(t)$ is the position of the moving liquid–solid interface. After all mathematical arrangements and operations, the solution of Eq. (17) verifying Eqs. (18)–(21), gives $\delta(t)$ as

$$\operatorname{erfc}(\lambda) - \frac{T_{\text{m}} - T_0}{T_{\text{mean}} - T_0} - \frac{2k_{\text{s}}(T_{\text{m}} - T_0)}{h(T_{\text{mean}} - T_0)(l - \delta(t))} \times \sum_{n=0}^{\infty}(-1)^n \xi_n \mathrm{e}^{-\xi_n^2 Fo_{\text{s}}} \sin\xi_n = \frac{\lambda}{Bi_{\text{m}} \cdot \text{Ste}} \tag{22}$$

where the following parameters has been used:

$$\text{Ste} = \frac{C_{p_{\text{l}}}(T_{\text{mean}} - T_0)}{L}$$

$$Fo_s = \frac{\alpha_s t}{(l-\delta(t))^2}$$

$$Bi_m = \frac{h(\alpha_l t)^{0.5}}{k_l}$$

$$\xi_n = \left(n+\frac{1}{2}\right)\pi$$

$$\lambda = \frac{\delta(t)}{2(\alpha_l t)^{0.5}}$$

For a given δ, Eq. (22) is solved to give time t. In order to verify the validity of the model, we compared the experimental results found by Zivkovic and Fujii [10] for calcium chloride hexahydrate ($CaCl_2 \cdot 6H_2O$) PCM slab of, $l = 0.01$ m, $T_m = 29.9$ °C, with the analytical results given by Eq. (22). The experimental results gave a time for complete melting of $t_{exp} = 68$ min, whereas for the same conditions ($T_{mean} = 60$ °C and $h = 16$ W/(m^2 K)) our model gives, $t_{analy} = 68.7$ min.

5. Case study

A complete solar installation situated at Lleida city in Catalunya, Spain, is studied. The SC is oriented $N \rightarrow S$, with an optimal inclination of 45°, $A_C = 1.9$ m^2, and $M_0 = 4$ L. A March's representative day has been considered for calculating all parameter's design and optimization. The collected solar irradiation is shown in Fig. 4. Thermal losses in water ducts between SC and SEST are neglected. Only the collector's characteristics as the caption area A_C, tube sectional area A_{cr} and SCs water charge M_{SC} are needed.

The first step is to optimize the water mass flow through the SC in order to extract the maximum work from the solar energy, as explained in Section 2. For this purpose, the optimal reduced temperature at each hour for the water going out of the SC, $\theta_{opt,j}$, is calculated by solving Eq. (10) for each value of the hourly solar irradiation $I_{g,j}$, shown in Fig. 4. Fig. 5 shows the result for $T_{opt,j} = \theta_{opt,j} \cdot T_{amb}$, the optimal temperature at each hour for the water going out the SC. Due to the stratification phenomena, the SCs input temperature could be considered as constant during all the irradiation period and equal to the ambient temperature T_{amb}.

Once $\theta_{opt,j}$ is know for each hour, the optimal water flow, $\dot{m}_{opt,w}$, is evaluated from Eq. (7). Fig. 6 shows the optimal water flow, $\dot{m}_{opt,w}$, at each hour as a function of time. From Figs. 5 and 6 it could be seen that SCs optimal output temperature reaches its maximum value of 372.5 K during 3 h, i.e., from 12 h to 15 h, when the optimal flow rate is an increasing function. This reaches a maximum value of 9.487 L/h from 17 h to 18 h. Integrating the curve

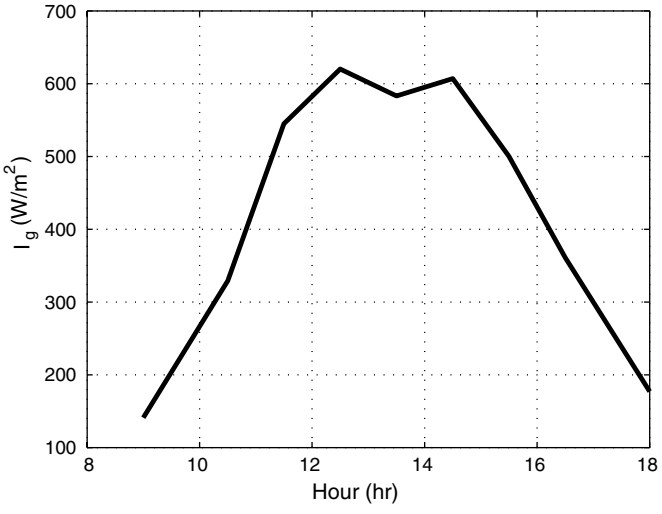

Fig. 4. Global solar irradiation variation during day March, 16th 2003 in Lleida (Spain).

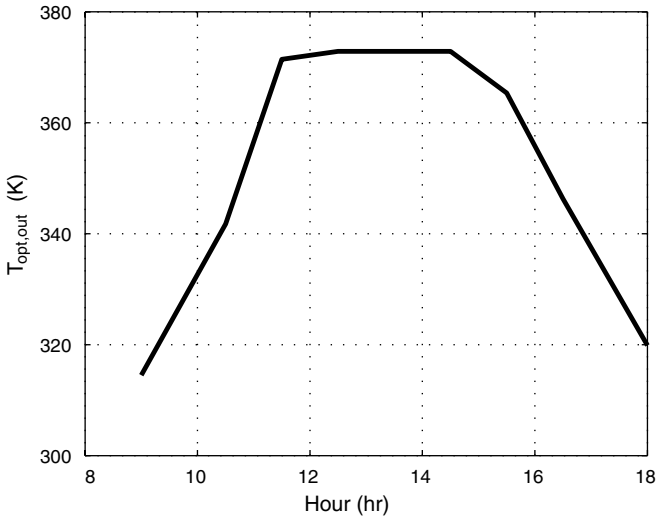

Fig. 5. SCs optimal output temperature variation during the day.

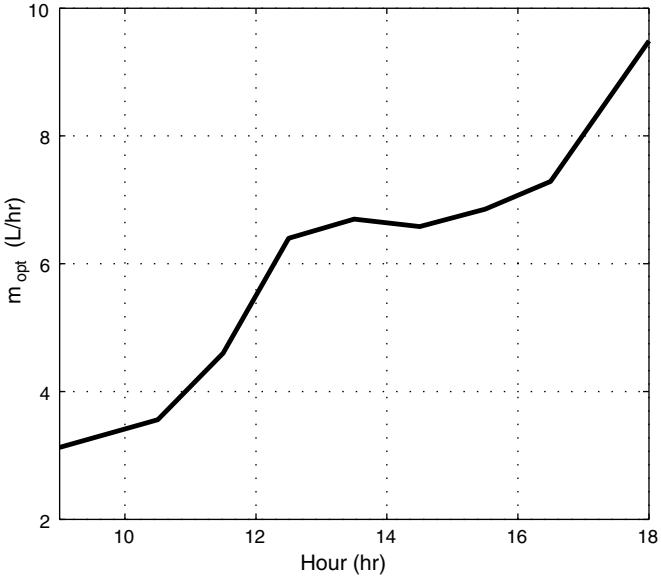

Fig. 6. SCs optimal flow rate variation during the day.

in Fig. 6, the optimal volume of water in SEST, V_{opt}, is found to be 55 L.

Once this value is found, next step consists on maximising the availability of the SEST, as explained in Section 3. First, the number of slabs, n, and the guess value for the temperature at which the thermo-physical properties of water are computed, T^k, are introduced. This allows for a determination of the hourly Reynolds number, Re_j, computed as

$$Re_j = \frac{\dot{m}_j}{\mu_w n \pi \left(\frac{D_h}{2}\right)} \tag{23}$$

where μ_w is the viscosity of water, n is the number of slabs and D_h is the hydraulic diameter calculated as

$$D_h = \frac{2an(l+a)}{a+2n(l+a)} \tag{24}$$

where a is the distance between two slabs and l is the thickness of each slab.

The hourly Nusselt number, Nu_j, can be calculated from the empirical correlation for convective flow through tubes [19]

$$Nu_j = 3.66 + \frac{0.065\left(\frac{D_h}{b}\right)Re_j Pr}{1+0.04\left(\frac{D_h}{b}Re_j Pr\right)^{0.667}}, \quad \text{if } Re < 2300 \tag{25}$$

$$Nu_j = \frac{\frac{f}{8}(Re_j - 1000)Pr}{1+12.7\left(\frac{f}{8}\right)^{0.5}\left(Pr^{0.667}-1\right)}, \quad \text{if } Re \geqslant 2300,$$

$$f = \left(0,790\ln(Re_j) - 1.64\right)^{-2} \tag{26}$$

where b is the slabs high and Pr is the Prandtl number:

$$Pr = \frac{C_p \mu_w}{k_w} \tag{27}$$

From the definition of the Nusselt number

$$Nu = \frac{hD_h}{k_w} \tag{28}$$

and the value obtained with Eqs. (25) and (26), the hourly heat transfer coefficient, h_j can be calculated. From expression (12), the hourly number of transfer unit, $N_{tu,j}$, can be calculated.

From Eq. (15) and the guess value T^k, the optimal melting temperature for the PCM is calculated. With the obtained value of $T_{m,opt}$ and Nu, the output temperature T_{out} is calculated with Eq. (11). From T_{in} and T_{out}, the temperature at which the thermo-physical properties of water are computed T^{k+1} is then re-calculated as $T^{k+1} = (T_{out} + T_{in})/2$ and compared with T^k. The process is repeated until the condition $|T^{k+1} - T^k| < \varepsilon$ is satisfied.

The information given by the number of transfer units, N_{tu}, is very important for designing. For instance it informs of whether n should be changed or not.

The fractional energy, Ψ, given by the melted PCM of a melting temperature, T_m, and recovered by the entering water is defined as the actual energy given by the PCM divided by the total energy, that is, $\Psi = (T_{mean} - T_m)/(T_{in} - T_m)$. The water's mean temperature bathing each PCMs hourly section is evaluated simply by $T_{mean} = (T_{out} + T_{in})/2$.

The other important key parameter for design in this problem is the melted thickness, $\delta(t)$, which is function of the thermal properties of the PCM, thickness and boundary conditions, this is, h and T_{mean}. This is evaluated by using Eq. (22).

Fig. 7 shows the variation of the optimal melting temperature of the PCM, $T_{m,opt}$, and the mean temperature of the water bathing the PCM slabs, T_{mean}, with the PCM slabs height during the first 6 h, i.e. 9–15 h. As the height of the PCM slab increase, $T_{m,opt}$ and T_{mean} decrease. Thus, for $l = 0.135$ m, $T_{m,opt} = 363$ K and $T_{mean} = 365$ K whereas for $l = 0.38$ m, $T_{m,opt} = 327$ K and $T_{mean} = 332$ K. From 15 h to 18 h and depending on the chosen PCMs melting temperature, a fractional energy, Ψ, will be given by the melted PCM to the entering water. Fig. 8 shows that for $l = 0.135$ m, $\Psi = 58.54\%$ and for $l = 0.38$ m, $\Psi = 25.49\%$.

In order to chose the optimal PCM, the irreversibility I_r defined as the energy not recovered by the PCM from entering water [20], has been evaluated. Considering Rubitherm PCM products [21] and from Fig. 9, for $T_{m,opt} = 327$ K, the recovered energy by the entering water during the 3 h is 612.18 kJ while the energy not recovered by water, i.e. the irreversibility, is 1836.54 kJ. However, for $T_{m,opt} = 363$ K, the recovered energy by the entering water is 561 kJ while the energy not recovered is 406 kJ. Thus, the irreversibility at $T_{m,opt} = 363$ K is 4.52 lower than the one at $T_{m,opt} = 327$ K. For this reason, the energy quality extracted at $T_{m,opt} = 363$ K is 4.52 times better than the energy extracted at $T_{m,opt} = 327$ K.

At the upper layer of height 0.136 m, the temperature of the water is $T_{mean} = 365$ K for almost 5 h. Eq. (22) suggests

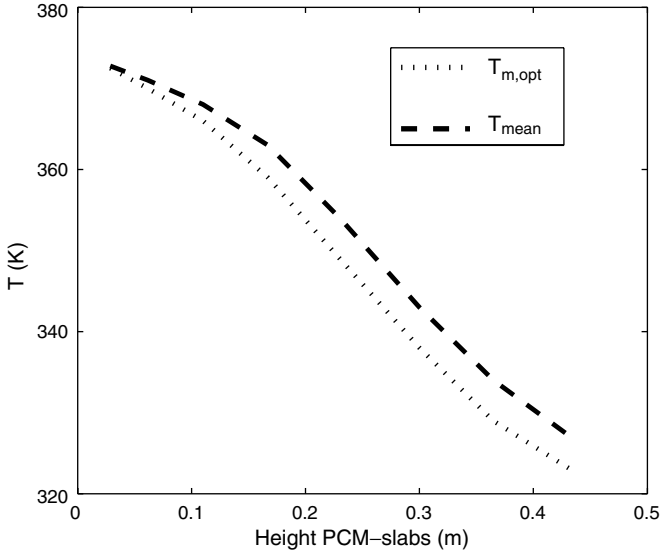

Fig. 7. Variation of PCMs optimal melting temperature and water's mean temperature bathing PCMs slabs with the PCMs slabs height.

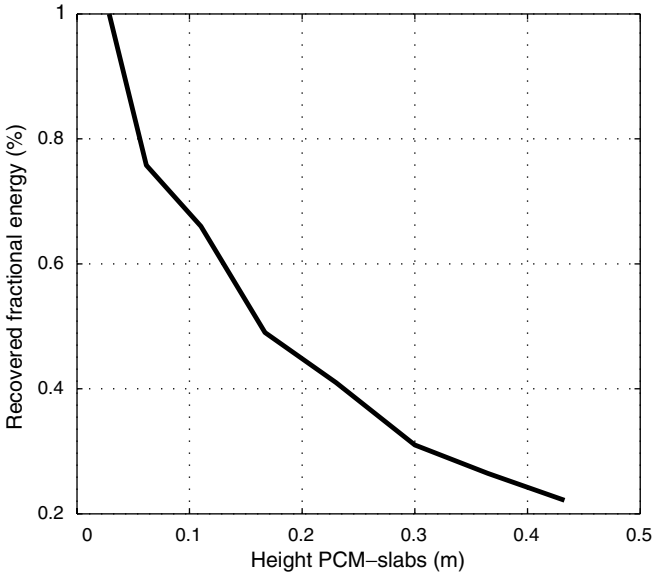

Fig. 8. Variation of the recovered fractional energy as a function of PCMs slabs height.

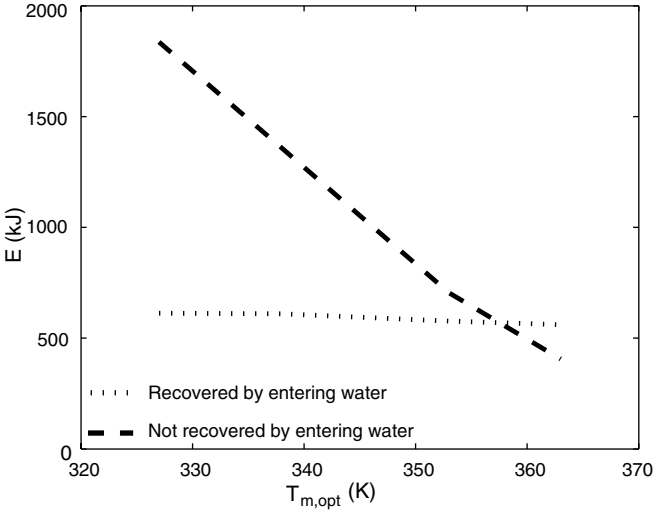

Fig. 9. Variation of recovered and not recovered energy with the chosen PCMs optimal temperature.

that l should not be greater than 0.003 m. With the aim of obtaining a square base tank, we find that the most acceptable design in this case corresponds to $n = 20$, and consequently $N_{tu} = 23.4$ and $h = 188\ \mathrm{W/m^2\,K}$. Moreover, for $n = 20$, N_{tu} and h remains nearly constant during all the day (i.e. $N = 9$ h). Fig. 10 shows the results obtained with Eq. (22) for the time evolution of the melted portion of PCM, for different PCMs melting temperature. As can be seen, the necessary time for complete melting is an increasing function of T_m. The calculated melting time values for four different Rubitherm PCMs of different melting temperatures T_m are 0.54 h for RT54 ($T_m = 327$ K), 0.856 h for RT65 ($T_m = 338$ K), 1.99 h for RT80 ($T_m = 353$ K) and 4.48 h for RT90 ($T_m = 363$ K).

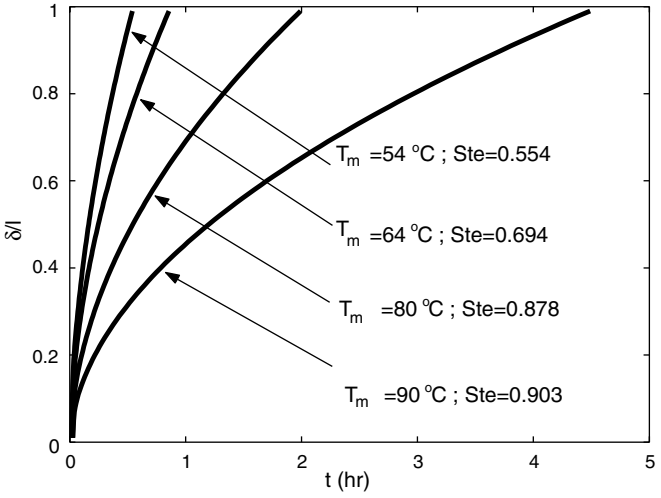

Fig. 10. Time evolution of the melted portion for different PCM.

6. Conclusion

A more general exergetic optimization of the whole solar energy installation has been carried out for a representative day of March in Lleida (Spain). It has been found that the optimal water volume is 55 L, for a SC of 1.9 m^2, inclined 45° and oriented $N \rightarrow S$. Also, the exergetic optimization study of the PCM-slabs–SEST gives optimal melting temperature. Results shows that T_m ranges between 327 K and 363 K. For each melting temperature corresponds a PCM-slabs height. Thus, for $T_m = 327$ K, $l = 0.38$ m when for $T_m = 363$ K, $l = 0.135$ m. The fractional energy, Ψ, function of T_m, given by the PCM-slabs to the entering water has been also examined. For $T_m = 363$ K, $\Psi = 58.54\%$ and for $T_m = 327$ K, $\Psi = 25.49\%$. The irreversibility is 406 kJ at $T_{m,opt} = 363$ K, while it is 1836.54 at $T_{m,opt} = 327$ K. Therefore, the energy to be recovered at $T_m = 363$ K is 4.52 times better from the quality point of view. The examination of the melting process in a PCM-slabs–SEST assembly shows that the maximal PCM-slabs thickness allowed is of about $2l = 0.006$ m. Thus, for $n = 20$ slabs, for $T_m = 327$ K (resp. $T_m = 363$ K) the SEST size is $0.4 \times 0.4 \times 0.46$ m (resp. $0.4 \times 0.4 \times 0.39$ m).

References

[1] H. Yoo, C.-J. Kim, C.W. Kim, Approximate analytical solutions for stratified thermal storage under variable inlet temperature, Sol. Energy 66 (1) (1998) 47–56.
[2] J.E.B. Nelson, A.R. Balakrishnan, S. Srinivasa Murthy, Experiments on stratified chilled-water tanks, Int. J. Refrig.-Rev. Int. Froid. 22 (1999) 216–234.
[3] J.E.B. Nelson, A.R. Balakrishnan, S. Srinivasa Murthy, Parametric studies on thermally studied chilled water storage systems, Appl. Therm. Eng. 19 (1999) 89–115.
[4] K. Lovegrove, A. Luzzi, H. Kreetz, A solar driven ammonia-based thermochemical energy storage system, Sol. Energy 67 (4–6) (1999) 309–316.

[5] H. Kreetz, K. Lovegrove, Theoretical analysis and experimental results of a 1 kW_{chem} ammonia synthesis reactor for a solar thermochemical energy storage system, Sol. Energy 67 (4–6) (1999) 287–296.
[6] K. Lovegrove, A. Luzzi, M. Mccann, O. Freitag, Exergy analysis of ammonia-based solar thermochemical power systems, Sol. Energy 66 (2) (1999) 103–115.
[7] F. Aghbalou, A. Touzani, M. Mada, M. Charia, A. Bernatchou, A parabolic solar collector heat pipe heat exchanger reactor assembly for cyclohexane's dehydrogenation: a simulation study, Renew. Energy 14 (1–4) (1998) 61–67.
[8] M. Esen, A. Durmus, A. Durmus, Geometric design of solar-aided latent heat store depending on various parameters and phase change materials, Sol. Energy 62 (1) (1998) 12–28.
[9] F. Aghbalou, F. Badia, J. Illa, Design and analysis of a thermal solar energy storage using PCM, FIER 2002 Proc. 2 (2002) 395–401.
[10] B. Zivkovic, I. Fujii, An analysis of isothermal phase change material within rectangular and cylindrical containers, Sol. Energy 70 (1) (2001) 51–61.
[11] U. Stritih, An experimental study of enhanced heat transfer in rectangular PCM thermal storage, Int. J. Heat Mass Transfer 47 (2004) 2841–2847.
[12] M.A. Rosen, I. Dincer, Exergy methods for assessing and comparing thermal storage systems, Int. J. Energy Res. 27 (2003) 415–430.
[13] I. Dincer, Evaluation and selection of energy storage systems for solar thermal applications, Int. J. Energy Res. 23 (1999) 1017–1028.
[14] J. Stephan, Uber die theorie der eisbildung, insbesondere uber die eisbildung im polarmeere, Ann. Phys. Chem. 42 (1891) 269–286.
[15] P. Lamberg, K. Sirén, Analytical model for melting in semi-infinite PCM storage with an internal fin, Heat Mass Transfer 39 (2003) 167–176.
[16] J. Bass, Cours de Mathematiques, vol. 2, Masson, 1961.
[17] A. Bejan, Extraction of exergy from solar collector under time varying conditions, Int. J. Heat Fluid Flow 3 (1982) 67.
[18] J.S. Lim, A. Bejan, J.H. Kim, Thermodynamics optimisation of phase change energy storage using two or more materials, J. Energy Resour. Technol.—Trans. ASME 114 (1992) 84–90.
[19] F. Kreith, M.S. Bohn, Principles of Heat Transfer, sixth ed., Thomson Learning Inc., 2001.
[20] D.C. Look Jr., H.J. Sauer Jr., Engineering Thermodynamics, SI ed., Van Nostrand Reinhold (International) Co. Ltd., 1986 (Chapter 10).
[21] Rubitherm GmbH. Available from: <http://www.rubitherm.com>.